Published in final edited form as:
Curr Eye Res. 2014 October ; 39(10): 1059–1067. doi:10.3109/02713683.2014.892997.

Choroidal Blood Flow Decreases with Age: An MRI Study

Oscar San Emeterio Nateras[1,2], **Joseph M. Harrison**[3], **Eric R. Muir**[1,3], **Yi Zhang**[1,2], **Qi Peng**[1,2,4], **Steven Chalfin**[3], **Juan E. Gutierrez**[2], **Daniel A. Johnson**[3], **Jeffrey W. Kiel**[3], and **Timothy Q. Duong**[1,2,3,5]

[1]Research Imaging Institute, University of Texas Health Science Center, San Antonio, TX, USA

[2]Department of Radiology, University of Texas Health Science Center, San Antonio, TX, USA

[3]Department of Ophthalmology, University of Texas Health Science Center, San Antonio, TX, USA

[4]Department of Radiology, Albert Einstein College of Medicine, and Montefiore Medical Center, Bronx, NY, USA

[5]South Texas Veterans Health Care System, San Antonio, TX, USA

Abstract

Purpose—To verify that a visual fixation protocol with cued eye blinks achieves sufficient stability for magnetic resonance imaging (MRI) blood-flow measurements and to determine if choroidal blood flow (ChBF) changes with age in humans.

Methods—The visual fixation stability achievable during an MRI scan was measured in five normal subjects using an eye-tracking camera outside the MRI scanner. Subjects were instructed to blink immediately after recorded MRI sound cues but to otherwise maintain stable visual fixation on a small target. Using this fixation protocol, ChBF was measured with MRI using a 3 Tesla clinical scanner in 17 normal subjects (24–68 years old). Arterial and intraocular pressures (IOP) were measured to calculate perfusion pressure in the same subjects.

Results—The mean temporal fluctuations (standard deviation) of the horizontal and vertical displacements were 29 ± 9 μm and 38 ± 11 μm within individual fixation periods, and 50 ± 34 μm and 48 ± 19 μm across different fixation periods. The absolute displacements were 67 ± 31 μm and 81 ± 26 μm. ChBF was negatively correlated with age (R =−0.7, p = 0.003), declining 2.7 ml/100 ml/min per year. There were no significant correlations between ChBF versus perfusion pressure, arterial pressure, or IOP. There were also no significant correlations between age versus perfusion pressure, arterial pressure, or IOP. Multiple regression analysis indicated that age was the only measured independent variable that was significantly correlated with ChBF (p = 0.03).

Conclusions—The visual fixation protocol with cued eye blinks was effective in achieving sufficient stability for MRI measurements. ChBF had a significant negative correlation with age.

Correspondence: Timothy Q. Duong, PhD, Department of Ophthalmology, University of Texas Health Science Center at San Antonio, 8403 Floyd Curl Dr, San Antonio, TX 78229, USA. duongt@uthscsa.edu.

DECLARATION OF INTEREST The authors report no conflicts of interest.

Keywords

Choroidal basal blood flow; eye tracking; high-resolution MRI; visual fixation

INTRODUCTION

Advancing age has a significant impact on retinal structure, physiology and function.[1–4] Age is a leading risk factor in age-related macular degeneration, glaucoma, and vascular occlusive diseases.[1,5–9] Under normal physiological conditions, blood flow (BF) in the retina is closely coupled to metabolism and is tightly regulated.[10] Various techniques such as laser Doppler flowmetry, indocyanine green angiography, blue-field entoptic technique, and laser speckle imaging, among others[11–16] have been used to study age-dependent BF changes in the retina. However, most optically based BF imaging techniques are limited to imaging the fovea or the optic nerve head, are confounded by media opacity if present (i.e. cataract and vitreous hemorrhage), and are qualitative or semi-quantitative which makes comparison across different subjects challenging.

Quantitative BF magnetic resonance imaging (MRI) of the retina has recently been demonstrated. In anesthetized animals, BF in the two (retinal and choroidal) circulations can be quantitatively imaged and choroidal blood flow (ChBF) is 8–10 times higher than retinal BF.[17–21] In awake humans, the challenges of BF MRI are eye motion and limited spatial resolution of clinical MRI systems. Visual fixation on a target with cued blinks has been used to minimize motion artifacts.[22,23] A small eye radiofrequency coil with tailored pulse sequences and parameters can be used to improve the signal-to-noise ratio.[22] Nonetheless, it is not yet possible to separately resolve retinal and choroidal BF in humans. Because choroid BF (ChBF) is 8–10 times higher than retinal BF,[17–21] ChBF dominates in human BF MRI measurement of the retina to date. ChBF measured by MRI has been reported under basal conditions,[24,25] hypercapnia,[24,26] and isometric exercise[27] in normal subjects and in patients with retinitis pigmentosa.[28] Reproducibility of BF MRI across multiple repeated scans and across multiple sections on the same subjects has also been established.[24] An advantage of BF MRI is that it provides tissue BF in the quantitative and classical unit of ml/100 ml/min enabling cross-subject comparison. MRI also provides a large field of view, allowing measurement of combined retinal and ChBF, and is not obstructed by media opacity. The disadvantages of BF MRI are its low spatiotemporal resolution and high cost compared to optical-based techniques.

The goals of the present study were to assess the visual fixation stability achievable with cued eye blinks for BF MRI measurements and to test the hypothesis that ChBF changes with age in humans.

METHODS

Evaluation of Visual Fixation Stability

All studies were performed with Institutional Review Board approval. Visual fixation stability of five self-declared healthy subjects (three males, two females, 24–40 years old)

was measured with an eye-tracker (ETL-500, ISCAN Inc., Woburn, MA), which used digitized video images of the corneal reflection of light from a small infrared diode and the pupil center to determine horizontal and vertical location of line of sight at 240 Hz with 0.1° angular resolution or 29.1 μm at the posterior retina. The horizontal and vertical channels of each subject were calibrated prior to measuring fixation stability by digitizing the *x–y* coordinates of a central point and 4 points at the corners of a 20×20 degree square around the central fixation cross.

The subjects were placed in a supine position outside the MRI scanner. The same custom-made head holder used for MRI was used to secure and stabilize their heads. Subjects were instructed to maintain stable visual Exation on a small black cross on a white background at a distance of 30 cm and blink immediately after data-acquisition sound cues from the playback of recorded MRI sounds. The subjects were trained to synchronize their eye-resting and fixation cycle with the scanner sound cues. Specifically, there were three distinct periods within each repetition cycle (4.6 s): (1) the 2-s spin-labeling period when high-pitch noises were made, (2) the 1.5 s delay time when the scanner was quiet, and (3) the 0.4 s data acquisition period when short-period, lower-pitch noises were made. Subjects were instructed to close their eyes and rest during spin labeling, open their eyes and fixate on the target during spin-labeling delay, and maintain stable visual Exation during data acquisition. The fixation target was the same configuration used in the scanner. Eye-tracking data were recorded for 20 fixation periods (1.5 min) from which 10 were randomly chosen for analysis. Three repeated trials were measured in each subject.

Angular amplitudes, as measured by the eye tracker, were converted to visual angle of the ocular excursion (1° = 291 μm)[29,30] and plotted as a function of time. For quantitative analysis, data during eye blinks were discarded to reduce motion artifacts (eye tracking was lost during blinks when eye lids were closed). A stable fixation period of 0.4 s was extracted and analyzed using MATLAB (MathWorks Inc., Natick, MA) codes. Three parameters were tabulated for horizontal and vertical movements separately: (1) the standard deviation of the amplitude was computed for every sample and then averaged, (2) the mean displacement from every sample was computed and then the standard deviation taken, and (3) the mean absolute displacement across all fixation period samples was computed.

MRI Experiments

MRI studies were performed on 17 self-declared healthy subjects (12 males, 5 females, 24–68 years old) with normal vision verified by an ophthalmologist. These subjects did not have any known cardiovascular diseases or take medications. A 3 Tesla whole-body MRI scanner (Achieva, Philips Healthcare, Best, Netherlands) equipped with an 80 mT/m gradient system, a commercial body RF coil for signal excitation, and a custom-made, receive-only oblique eye coil of 6 cm in diameter were used. The diameter and shape of the eye-coil were optimized for signal-to-noise ratio at the posterior pole of the adult human retina. Subjects were positioned supine with the head in a custom-made head holder and were instructed to synchronize their eye-blinking and fixation cycle with the scanner noise during the arterial spin-labeling (ASL) scan, in the same way as they did in the visual fixation stability test

outside of the scanner. A central axial slice bisecting the optic nerve head and fovea was imaged to minimize partial volume effect due to the retinal curvature.

BF was imaged using the pseudo-continuous ASL technique as previously described[31] using a 2 s labeling duration, 1.5 s post-labeling delay, and with the labeling plane set at 7 cm inferior to the imaging plane at the level of the internal carotid artery. Background suppression employed two inversion pulses at 2061 and 3405 ms after the initial saturation pulse, which was placed before the labeling. For image acquisition, a single-shot Turbo Spin Echo (TSE) sequence was used with a repetition/echo time (TR/TE) of 4.6 s/30 ms, a 6 mm slice thickness, 12.8 kHz bandwidth, TSE factor of 28, a field of view = 50×43mm, and matrix size = 100×53, (in plane resolution of 500×800 μm). The higher spatial resolution was placed along the readout direction, perpendicular to the posterior retina. Half-Fourier acquisition (52.5%) and linear profile ordering were used along the phase-encode direction, leading to a total TSE echo train length of 343 ms. Spatially-selective gradients were applied along with RF refocusing pulses to avoid aliasing artifacts along the phase-encode direction.[31] Label and control images were acquired alternately with a temporal resolution of 9.2 s per paired image. In addition, a reference scan with TR = 15 s was used to derive M_0 for BF quantification. The mean basal BF was analyzed from the region of interest (ROI) in ml/100 ml/min. Each block of BF MRI acquisition consisted of 20 pairs of images and 2–5 blocks were acquired on each subject.

All MRI images from each scan were first co-registered using a custom algorithm written in MATLAB, as previously described in detail.[32] Quantitative BF maps in units of ml/100 ml/min were calculated using the following equation:[24,33]

$$BF=\frac{6000}{2\cdot\lambda\cdot\alpha\cdot\alpha_{inv}\cdot T_{1,\,blood}}\cdot\frac{\Delta M_{ASL}}{M_o}\cdot e^{T1/T_{1,\,blood}}\cdot e^{TE/T_{2\,blood}},$$

where ΔM_{ASL} is the difference of the control and label images. λ is the water content of blood in ml water/ml arterial blood (0.85).[34] The blood relaxation times $T_{1,blood}$ and $T_{2,blood}$ are 1700 and 275 ms.[35,36] α was the arterial spin-labeling efficiency and was assumed to be 0.85,[37] with the use of inversion giving the factor of 2. α_{inv} was 0.83 which corrected for the loss of perfusion signal due to the two background suppression pulses.[38] The constant 6000 is to convert the units from ml blood/ml/s to ml blood/100 ml/min. TI is the post-labeling delay time and M_0 is the equilibrium signal intensity of the vitreous calculated from the reference scan corrected for scaling factors and amplification differences with the ASL sequences. The equilibrium signal intensity of the vitreous was used as an intensity reference for pure water, avoiding the use of unknown retina– blood partition coefficient in the quantitative BF calculation.

To objectively quantify BF data and minimize the partial volume effect, automated profile analysis was performed to generate the BF profiles across the thickness of the retina and along the length of the retina.[39] BF values for the choroidal vasculature were taken at the peaks of the projection profiles. Four ROIs outlining the posterior retina: Peripheral temporal region (PTR), foveal temporal region (FTR), optic nerve head region (ONHR), and peripheral nasal region (PNR) with the size of 4 mm along the retina and 0.7 to 0.8 mm

across the choroidal thickness were used to obtain the BF signal time courses and averaged BF values.

After each subject underwent BF MRI, their intraocular pressure (IOP) was measured with a tonopen and their brachial artery blood pressure was measured with an automated sphyngomanometer in the supine position outside the scanner. Mean arterial pressure (MAP) was calculated as diastolic pressure + 0.42 • (systolic pressure – diastolic pressure).[40,41] Supine ocular perfusion pressure (OPP) was calculated as MOAP – IOP, where the mean ophthalmic arterial blood pressure (MOAP) = 0.84 • MAP in the supine position.[42,43]

Statistical Analysis

Linear regression between any two of the measured parameters (ChBF, age, OPP, MAP, IOP) was analyzed. Multiple regression analysis was done with ChBF as the dependent variable for the four ROIs and age, OPP, MAP, and IOP as the independent variables. Correlation coefficients and *p* values were obtained. Peak BF values from the ChBF profiles of two arbitrary age groups (24–37 years ($n = 9$) and 38–68 years ($n = 8$)) were compared by an unpaired *t*-test (two-tailed). A p value<0.05 was taken to be statistically significant.

RESULTS

The eye tracker was calibrated and verified on an artificial eye to have a resolution of 29.1μm (data not shown). The amplitudes of the vertical and horizontal eye movements from single-subject eye-tracking measurements during the visual fixation protocol with cued blinks are shown in Figure 1. All subjects were able to achieve stable visual fixation during the data acquisition period within each TR cycle, and the 4.6 s resting-fixation cycle was comfortable for all subjects studied. The three tabulated parameters were as followed: (1) the temporal standard deviations of displacement during a single fixation period were 29 ± 9μm (horizontal direction) and 38 ± 11μm (vertical direction) (mean ± SD, N = 5, Figure 2A). (2) The temporal standard deviations of displacement across multiple fixation periods were 50 ± 34 μm and 48 ± 19 μm (Figure 2B). (3) The mean absolute displacements of the eye position from the mean reference point were 67 ± 31 μm and 81 ± 26 μm (Figure 2C).

Time-loop movies of the time-series MRI images were free from significant movement artifacts. Co-registration was successful in correcting minor drift and movement in most scans. A small number of images (~3%) showed significant eye movement during data acquisition and were discarded. Figure 3 shows a representative anatomical MRI image, a BF map, and the ChBF profile across the retinal thickness and along the retina. BF was highest in the posterior choroid and slightly lower in the optic nerve head. In most subjects, two BF layers (retinal and choroidal) are visible around the fovea but became less apparent away from the central retina. The averaged profile along the length of the retina shows the retinal BF layer as a slight shoulder of the high BF choroidal peak. Retinal BF however was not analyzed because of low signal-to-noise ratio. Note that the peak BF value in Figure 3D likely reflects that of the fovea (free of retinal vessels) and thus mostly ChBF (albeit some partial volume).

With the ROI centered at the fovea, ChBF was negatively correlated with age (BF = 295 – 2.7 age, $R = -0.7$, $p = 0.003$, $N = 15$, Figure 4), declining 2.7 ml/ 100 ml/min per year. These results were obtained with exclusion of the two open symbols, which represented two subjects with severe myopia. Their inclusion also yielded significant, albeit weaker, correlation ($R = -0.54$, $p = 0.03$, $N = 17$). These results suggest that BF in severe myopia was markedly reduced.

With the optic nerve head ROI (labeled as ROI b in Figure 4 inset), ChBF was negatively correlated with age (BF = 112 – 0.94 age, $R = -0.5$, $p = 0.05$, $N = 15$). There were however no significant age-dependent effects for the periphery ROIs (labeled as ROI c and d in Figure 4 inset). Data from ROIs b, c and d are not plotted.

Figure 5 shows the correlations of other parameters. There was no significant correlation between BF with OPP ($R = 0.13$, $p = 0.6$), MAP ($R = 0.14$, $p = 0.6$), or IOP ($R = -0.15$, $p = 0.9$). Age did not have any significant correlations with OPP ($R = 0.14$, $p = 0.6$), MAP ($R = 0.18$, $p = 0.49$), or with IOP ($R = 0.04$, $p = 0.9$). Multiple regression analysis in which ChBF was taken as the dependent variable, and age, OPP, MAP, and IOP as independent variables, also revealed statistical significance ($R = -0.8$, $p<0.03$, $N = 15$, for ROI “a”). Age was the only independent variable that was significant but only for ROI “a” ($p = 0.006$) and for the ONH ROI ($p<0.05$), while OPP, MAP and IOP were not significant ($p = 0.8$, $p = 0.9$, and $p = 0.9$, respectively).

When arbitrarily dividing subjects into two groups (24–37-year-olds and 38–68-year-olds), peak BF was significantly higher in the younger group (270 ± 98 ml/100 ml/min) than the older group (161 ± 54 ml/100 ml/min) ($p<0.001$) (Figure 6).

DISCUSSION

Visual Fixation Stability

BF MRI measurements take several minutes to perform and thus require visual fixation stability over time. BF MRI of the retina is particularly susceptible to motion artifacts because the BF signal is dependent on subtraction between two separate images (with and without labeling) and the thin retina is bounded by the sclera and vitreous which have different signal intensities than the retina. A visual fixation protocol for lamina-specific anatomic MRI of the human retina has been previously reported,[22] where the temporal displacement relative to a reference point was 73 μm horizontal and 120 μm vertical displacements (SD of the amplitude) for a comfortable blinking period of 6–8 s. In the current study, the visual fixation stability protocol was improved, taking advantage of the relatively short data acquisition window for each ASL TR-cycle. The improvement was, in part, due to longer eye-resting and blinking durations and a shorter fixation duration (2 s) for subjects during each 4.6 s TR-cycle. These data are comparable to previous measures of fixation stability (e.g. standard deviations of 31 mm (horizontal) and 24 μm (vertical) during 12.8 s visual fixation periods).[44]

A limitation of this study is that it is challenging for BF MRI to resolve the retinal and choroidal BF layers and the avascular layer in between. This is because: (i) the spatial

resolution of this study is 500 × 800 mm and the human retinal thickness is only 700 mm including the choroid,[22] (ii) the avascular layer separating the retinal and choroidal vasculature is ~100 mm and the retinal BF may be overshadowed by the choroidal BF which is many times higher,[17,19] (iii) eye motion, and (iv) low signal-to-noise ratios. In animal models, it is possible to separately image the retinal and ChBF layer, and the avascular layer in between.[17–21] Similarly, the foveal pit (~500 mm) has no retinal vessels but has high choroidal flow. We have not yet achieved the spatial resolution to visualize the foveal pit at this time. Future studies will need to improve spatial resolution and sensitivity in human BF MRI.

Choroidal Blood Flow Changes with Age

OPP, MAP, and IOP showed trends with age but did not reach statistical significance, likely because of the small sample size. Previous studies have found OPP, MAP, and IOP increased with age in larger sample sizes.[12,13,16] Those studies also reported that increased OPP and MAP correlated negatively with retinal leukocyte velocity[12] and laser Doppler flowmetry measures of ChBF and blood volume.[13] However, they also found using multiple regressions including age, MAP, and OPP, that choroidal hemodynamics only significantly correlated with age. These findings suggest that possible changes of MAP or OPP with age have little effect on ocular perfusion.

Reproducibility of BF MRI across multiple repeated scans and across multiple sections on the same subjects has also been described.[24] ChBF peaked in the foveal region and dropped off in human retinas[24] and baboon retinas.[45] Previous measurement of regional choroidal BF in monkeys using fluorescent microspheres showed similar BF profiles, peaking around the fovea.[46] Our ChBF is in general agreement with previous MRI reports in human adults.[24,25] However, there are no published data with similar quantitative units using MRI or other methods to allow quantitative comparison with our BF age-dependent effects. A major finding of this study is that MRI BF was negatively correlated with age, declining 2.7 ml/100 ml/min per year. Although we assumed the relation is linear and applied linear regression analysis, BF may not change linearly with age. Indeed, our results suggest that BF drops off faster in the younger age range.

The number of choroidal arterioles and the fuorescent intensity in the macular region were observed to decrease with age by indocyanine green angiography.[11] Dye-filling was delayed, vessels were thickened and ran a straight course (instead of tortuous) with reduced branching and the watershed zone was blurred in older subjects.[11] Although the number of choroidal veins was not correlated with age, an increase in size of patch-like (hypofluorescent) structures was present and remained longer with age at the late venous phase. These hypofluorescent regions may result from the dye-filling delay or irregular dye filling into the choriocapillaries, augmented choroidal interstitial tissue developed from vascular thinning, and some angiographic blockages over the choroid, such as hyperpigmentation at the retinal pigment epithelium. These findings indicated that there are significant structural changes associated with age. Similarly, an age-related decrease of the foveolar choroidal circulation was detected by laser Doppler flowmetry.[13] Reduced

choroidal BF was attributed mainly to an age-related decrease in choroidal volume as the result of decreased density and lumen diameter of the choriocapillaries.[4]

With the blue-field entoptic technique, Grunwald et al.[12] reported a significant negative correlation between retinal leukocyte velocity and age, and between leukocyte density and age. They suggested that the drop in retinal macular BF might be a consequence of age-related structural changes that occur in the retina, such as an age-related decrease in number of photoreceptors and ganglion cells in humans. For example, Gao and Hollyfield[47] reported a 16% decrease in number of ganglion cells and Song et al.[48] found a significant decrease in cone photoreceptor packing density with age at distances less than 0.5 mm from the center of the fovea, but not at 0.9 mm.

Results using color Doppler imaging are more variable. There is support for a progressive alteration of orbital vascular parameters with age,[15] decreasing 9.9% per decade in central retinal artery BF velocities and increasing 4.9% per decade in the resistive index.[49] By contrast, William et al.[50] found an increase in the central retinal artery resistive index with age but no correlations in blood velocities in the central retinal artery and vein with age. Harris et al.[51] found no correlation between central retinal artery flow velocity and age. Gillies et al.[52] reported an increase of peak systolic velocity in the central retinal artery with age.

The present study measured BF in a supine position whereas most other techniques measured BF in a sitting position. In a study of pulsatile ocular BF (POBF), Ravalico et al.[16] found a significant correlation between POBF decline and age in the sitting position but only a trend in the supine position. Considering the supine position, several factors could bring about modification in the POBF, such as an increase in IOP secondary to higher episcleral venous pressure and intraocular volume, an extension of the length of the diastolic phase of the ocular pulse caused by a decrease in heart rate, or a change of blood pressure in the ophthalmic artery. It is possible that young people are better able to adjust to the abrupt increase in ophthalmic artery blood pressure when changing to the supine position. If so, it is possible MRI BF underestimated the age-dependent effects because the measurements were taken in supine position. In other words, younger subjects may maintain a normal MOAP even in supine posture but a slight increase in IOP could decrease their ChBF. In contrast, older subjects may not regulate their MOAP as well and so an increase in MOAP may occur in supine posture and counter balance the increase in IOP tending to increase their ChBF. BF MRI data could only provide a correlation, but could not address whether ChBF decline is the cause or the effect of choroidal physiological changes with age.

CONCLUSION

Cued visual fixation on a target achieved adequate stability for BF MRI measurement. Choroidal BF negatively correlated with age, declining 2.7 ml/100 ml/min per year. Such decrease in ocular BF could impair delivery of oxygen and nutrients, and removal of metabolic waste, making the retina more susceptible to diseases. Future studies will aim to improve spatial resolution and sensitivity to enable separate measurements of retinal and

choroidal BF in humans, to translate MRI techniques available on animals[53–55] to humans, as well as to apply BF MRI to investigate retinal diseases.

Acknowledgments

This work was supported in part by a Clinical Translational Science Award Pilot Grant (parent grant UL1RR025767), NIH/NEI (R01 EY021179, EY014211, EY021173, EY018855, and EY09702), and Department of Veterans Affairs MERIT awards.

REFERENCES

1. Cavallotti, C.; Cerulli, L. Age-related changes of the human eye. Vol. ch. 1. Humana Press; Totowa (NJ): 2008. p. 1
2. Pauleikhoff D, Chen JC, Chisholm IH, Bird AC. Choroidal perfusion abnormality with age-related Bruch's membrane change. Am J Ophthalmmol. 1990; 109:211–217.
3. Jablonski MM, Iannaccone A, Reynolds DH, Gallaher P, Allen S, Wang XF, Reiner A. Age-related decline in VIP-positive parasympathetic nerve fibers in the human submacular choroid. Invest Ophthalmol Vis Sci. 2007; 48:479–485. [PubMed: 17251439]
4. Ramrattan RS, van der Schaft TL, Mooy CM, de Bruijn WC, Mulder PG, de Jong PT. Morphometric analysis of Bruch's membrane, the choriocapillaris, and the choroid in aging. Invest Ophthalmol Vis Sci. 1994; 35:2857–2864. [PubMed: 8188481]
5. Seddon JM, Chen CA. The epidemiology of age-related macular degeneration. Internat Ophthalm Clinics. 2004; 44:17–39.
6. Le A, Mukesh BN, McCarty CA, Taylor HR. Risk factors associated with the incidence of open-angle glaucoma: the visual impairment project. Invest Ophthalmol Vis Sci. 2003; 44:3783–3789. [PubMed: 12939292]
7. Chen PP. Risk and risk factors for blindness from glaucoma. Curr Opin Ophthalmol. 2004; 15:107–111. [PubMed: 15021221]
8. Emre M, Orgul S, Gugleta K, Flammer J. Ocular blood flow alteration in glaucoma is related to systemic vascular dysregulation. Brit J Ophthalmol. 2004; 88:662–666. [PubMed: 15090420]
9. Wong TY, Klein R, Sharrett AR, Manolio TA, Hubbard LD, Marino EK, et al. The prevalence and risk factors of retinal microvascular abnormalities in older persons: the cardiovascular health study. Ophthalmology. 2003; 110:658–666. [PubMed: 12689883]
10. Pournaras CJ, Rungger-Brandle E, Riva CE, Hardarson SH, Stefansson E. Regulation of retinal blood flow in health and disease. Prog Retin Eye Res. 2008; 27:284–330. [PubMed: 18448380]
11. Ito YN, Mori K, Young-Duvall J, Yoneya S. Aging changes of the choroidal dye filling pattern in indocyanine green angiography of normal subjects. Retina. 2001; 21:237–242. [PubMed: 11421013]
12. Grunwald JE, Piltz J, Patel N, Bose S, Riva CE. Effect of aging on retinal macular microcirculation: a blue field simulation study. Invest Ophthalmol Vis Sci. 1993; 34:3609–3613. [PubMed: 8258519]
13. Grunwald JE, Hariprasad SM, DuPont J. Effect of aging on foveolar choroidal circulation. Arrch Ophthalmol. 1998; 116:150–154.
14. Embleton SJ, Hosking SL, Roff Hilton EJ, Cunliffe IA. Effect of senescence on ocular blood flow in the retina, neuroretinal rim and lamina cribrosa, using scanning laser Doppler flowmetry. Eye. 2002; 16:156–162. [PubMed: 11988816]
15. Ehrlich R, Kheradiya NS, Winston DM, Moore DB, Wirostko B, Harris A. Age-related ocular vascular changes. Graefe's archive for clinical and experimental ophthalmology. Graefes Arch Clin Exp Ophthalmol. 2009; 247:583–591. [PubMed: 19084984]
16. Ravalico G, Toffoli G, Pastori G, Croce M, Calderini S. Age-related ocular blood flow changes. Invest Ophthalmol Vis Sci. 1996; 37:2645–2650. [PubMed: 8977478]
17. Muir ER, Duong TQ. MRI of retinal and choroid blood flow with laminar resolution. NMR Biomed. 2011; 24:216–223. [PubMed: 20821409]

18. Muir ER, Renteria RC, Duong TQ. Reduced ocular blood flow as an early indicator of diabetic retinopathy in a mouse model of diabetes. Invest Ophthalmol Vis Sci. 2012; 53:6488–6494. [PubMed: 22915034]
19. Li G, De La Garza B, Shih YY, Muir ER, Duong TQ. Layer-specific blood-flow MRI of retinitis pigmentosa in RCS rats. Exp Eye Res. 2012; 101:90–96. [PubMed: 22721720]
20. Muir ER, De La Garza B, Duong TQ. Blood flow and anatomical MRI in a mouse model of retinitis pigmentosa. Magn Reson Med. 2013; 69:221–228. [PubMed: 22392583]
21. Lavery WJ, Muir ER, Kiel JW, Duong TQ. Magnetic resonance imaging indicates decreased choroidal and retinal blood flow in the DBA/2J mouse model of glaucoma. Invest Ophthalmol Vis Sci. 2012; 53:560–564. [PubMed: 22205612]
22. Zhang Y, Nateras OS, Peng Q, Kuranov RV, Harrison JM, Milner TE, Duong TQ. Lamina-specific anatomical magnetic resonance imaging of the human retina. Invest Ophthalmol Vis Sci. 2011; 52:7232–7237. [PubMed: 21828153]
23. Berkowitz BA, McDonald C, Ito Y, Tofts PS, Latif Z, Gross J. Measuring the human retinal oxygenation response to a hyperoxic challenge using MRI: eliminating blinking artifacts and demonstrating proof of concept. Magn Reson Med. 2001; 46:412–416. [PubMed: 11477648]
24. Peng Q, Zhang Y, Nateras OS, van Osch MJ, Duong TQ. MRI of blood flow of the human retina. Magn Reson Med. 2011; 65:1768–1775. [PubMed: 21590806]
25. Maleki N, Dai W, Alsop DC. Blood flow quantification of the human retina with MRI. NMR Biomed. 2011; 24:104–111. [PubMed: 20862658]
26. Maleki N, Alsop DC, Dai W, Hudson C, Han JS, Fisher J, Mikulis D. The effect of hypercarbia and hyperoxia on the total blood flow to the retina as assessed by magnetic resonance imaging. Invest Ophthalmol Vis Sci. 2011; 52:6867–6874. [PubMed: 21447683]
27. Zhang Y, San Emeterio Nateras O, Peng Q, Rosende CA, Duong TQ. Blood flow MRI of the human retina/choroid during rest and isometric exercise. Invest Ophthalmol Vis Sci. 2012; 53:4299–4305. [PubMed: 22661466]
28. Zhang Y, Harrison JM, Nateras OS, Chalfin S, Duong TQ. Decreased choroidal blood flow in retinitis pigmentosa as measured by MRI. Doc Ophthalmol. 2013; 126:187–197. [PubMed: 23408312]
29. Wyszecki, Gn; Stiles, WS. Color science: concepts and methods, quantitative data and formulas. Wiley; New York (NY): 1967. p. 227
30. Le Grand, Y. Light, colour and vision. English, 2nd ed.. Chapman & Hall; London: 1968. p. 50-51.
31. Chalela JA, Alsop DC, Gonzalez-Atavales JB, Maldjian JA, Kasner SE, Detre JA. Magnetic resonance perfusion imaging in acute ischemic stroke using continuous arterial spin labeling. Stroke. 2000; 31:680–687. [PubMed: 10700504]
32. Muir ER, Duong TQ. Layer-specific functional and anatomical mri of the retina with passband balanced SSFP. Magn reson Med. 2011; 66:1416–1421. [PubMed: 21604296]
33. van Osch MJ, Teeuwisse WM, van Walderveen MA, Hendrikse J, Kies DA, van Buchem MA. Can arterial spin labeling detect white matter perfusion signal? Magn Reson Med. 2009; 45:1155–1161.
34. Herscovitch P, Raichle ME. What is the correct value for the brain–blood partition coefficient for water? J Cereb Blood Flow Metab. 1985; 5:65–69. [PubMed: 3871783]
35. Lu H, Clingman C, Golay X, van Zijl PC. Determining the longitudinal relaxation time (T1) of blood at 3.0 Tesla. Magn Reson Med. 2004; 52:679–682. [PubMed: 15334591]
36. Stanisz GJ, Odrobina EE, Pun J, Escaravage M, Graham SJ, Bronskill MJ, Henkelman RM. T1, T2 relaxation and magnetization transfer in tissue at 3T. Magn Reson Med. 2005; 54:507–512. [PubMed: 16086319]
37. Wu WC, Fernandez-Seara M, Detre JA, Wehrli FW, Wang J. A theoretical and experimental investigation of the tagging efficiency of pseudocontinuous arterial spin labeling. Magn Reson Med. 2007; 58:1020–1027. [PubMed: 17969096]
38. Garcia DM, Duhamel G, Alsop DC. Efficiency of inversion pulses for background suppressed arterial spin labeling. Magn Reson Med. 2005; 54:366–372. [PubMed: 16032674]

39. Cheng H, Nair G, Walker TA, Kim MK, Pardue MT, Thulé PM, et al. Structural and functional MRI reveals multiple retinal layers. Proc Natl Acad Sci USA. 2006; 103:17525–17530. [PubMed: 17088544]
40. Longo A, Geiser MH, Riva CE. Posture changes and subfoveal choroidal blood flow. Invest Ophthalmol Vis Sci. 2004; 45:546–551. [PubMed: 14744897]
41. Kaeser P, Orgul S, Zawinka C, Reinhard G, Flammer J. Influence of change in body position on choroidal blood flow in normal subjects. Brit J Ophthalmol. 2005; 89:1302–1305. [PubMed: 16170121]
42. Sayegh FN, Weigelin E. Functional ophthalmodynamometry. Comparison between dynamometry findings of healthy subjects in sitting and supine positions. Internat J Ophthalmol. 1983; 187:196–201.
43. Sayegh FN, Weigelin E. Functional ophthalmodynamometry. Comparison between brachial and ophthalmic blood pressure in sitting and supine position. Angiology. 1983; 34:176–182. [PubMed: 6829979]
44. Kosnik W, Fikre J, Sekuler R. Visual fixation stability in older adults. Invest Ophthalmol Vis Sci. 1986; 27:1720–1725. [PubMed: 3793400]
45. Zhang Y, Wey HY, San Emeterio Nateras O, Peng Q, De La Garza BH, Duong TQ. Anatomical, blood oxygenation level-dependent, and blood flow MRI of nonhuman primate (baboon) retina. Magn Reson Med. 2011; 66:546–554. [PubMed: 21360746]
46. Nork TM, Kim CB, Shanmuganayagam D, Van Lysel MS, Ver Hoeve JN, Folts JD. Measurement of regional choroidal blood flow in rabbits and monkeys using fluorescent microspheres. Arch Ophthalmol. 2006; 124:860–868. [PubMed: 16769840]
47. Gao H, Hollyfield JG. Aging of the human retina. Differential loss of neurons and retinal pigment epithelial cells. Invest Ophthalmol Vis Sci. 1992; 33:1–17. [PubMed: 1730530]
48. Song H, Chui TY, Zhong Z, Elsner AE, Burns SA. Variation of cone photoreceptor packing density with retinal eccentricity and age. Invest Ophthalmol Vis Sci. 2011; 52:7376–7384. [PubMed: 21724911]
49. Groh MJ, Michelson G, Langhans MJ, Harazny J. Influence of age on retinal and optic nerve head blood circulation. Ophthalmology. 1996; 103:529–534. [PubMed: 8600432]
50. Williamson TH, Lowe GD, Baxter GM. Influence of age, systemic blood pressure, smoking, and blood viscosity on orbital blood velocities. Brit J Ophthalmol. 1995; 79:17–22. [PubMed: 7880783]
51. Harris A, Harris M, Biller J, Garzozi H, Zarfty D, Ciulla TA, Martin B. Aging affects the retrobulbar circulation differently in women and men. Arch Ophthalmol. 2000; 118:1076–1080. [PubMed: 10922201]
52. Gillies WE, Brooks AM, Scott M, Ryan L. Comparison of colour Doppler imaging of orbital vessels in elderly compared with young adult patients. Austr New Zeal J Ophthalmol. 1999; 27:173–175.
53. Duong TQ, Pardue MT, Thule PM, Olson DE, Cheng H, Nair G, et al. Layer-specific anatomical, physiological and functional MRI of the retina. NMR Biomed. 2008; 21:978–996. [PubMed: 18792422]
54. Duong TQ. Magnetic resonance imaging of the retina: a brief historical and future perspective. Saudi J Ophthalmol. 2001; 25:137–143. [PubMed: 23960915]
55. Duong TQ, Muir ER. Magnetic resonance imaging of the Retina. Jpn J Ophthalmol. 2009; 53:352–367. [PubMed: 19763752]

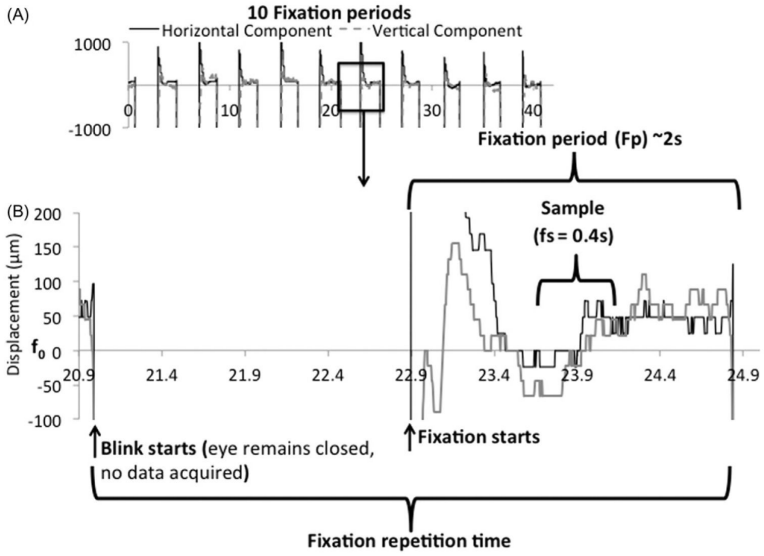

FIGURE 1.

(A) Ten fixation periods using the visual fixation protocol with cued blinks in one subject. Vertical and horizontal eye movements measured using the eye-tracking device are shown. The large vertical deflections are eye blinks where tracking of the cornea was lost when eyelids were closed. (B) The fixation period lasted ~2 s. The sample evaluated over the duration (fs) of 0.4 s is displayed. The resolution of the eye tracker is 29.1 mm.

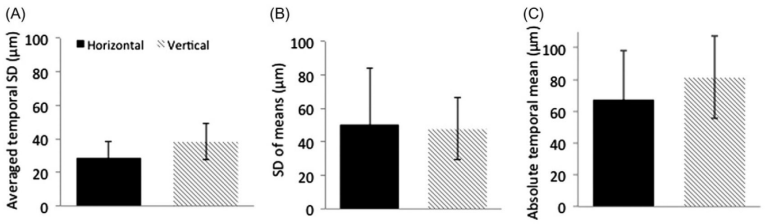

FIGURE 2.

(A) Fluctuation within a single fixation sample was calculated by averaging the temporal standard deviations of every fixation period (10 per trial) yielding 29 ± 9 mm and 38 ± 11 μm for the horizontal and vertical displacements, respectively. (B) Fluctuation across multiple fixation samples was calculated by taking the temporal standard deviations across 10 fixation periods samples yielding 50 ± 34 μm and 48 ± 19 μm for the horizontal and vertical displacements, respectively. (C) The absolute mean difference of the eye position from a mean reference point was 67 ± 31 μm and 81 ± 26 μm for the horizontal and vertical displacements, respectively. Each trial consisted of 10 fixation samples and 2–3 trials were analyzed for each of the 5 subjects. Error bars are ±SD.

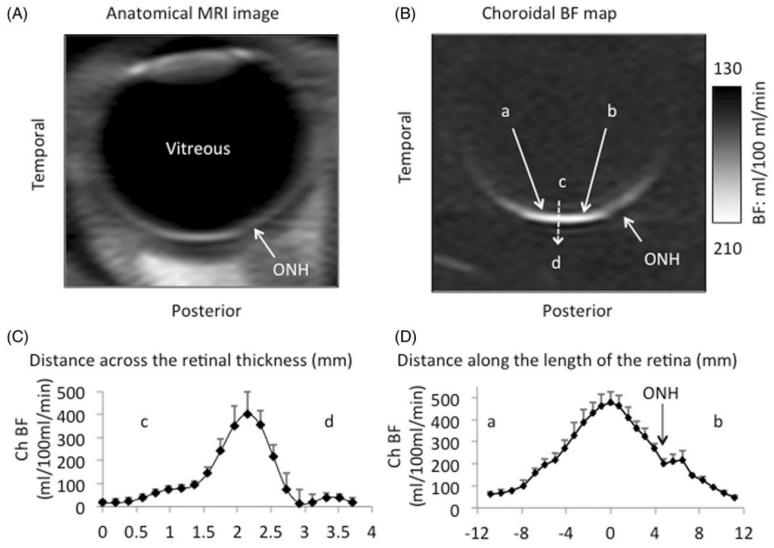

FIGURE 3.

(A) Anatomical MRI and (B) choroidal blood flow image of the human retina from one subject. Blood flow was high around the macula and dropped off peripherally. Four ROIs were evaluated: (1) Peripheral temporal region (PTR), (2) Foveal region (FTR), (3) Optic nerve head region (ONHR), and (4) Peripheral nasal region (PNR) (C) Mean BF profile across the retina from c to d, averaged along point a to b (4 mm). The choroidal blood flow was calculated using the peak value. (D) Mean choroidal blood flow from point a (temporal) to b (nasal).

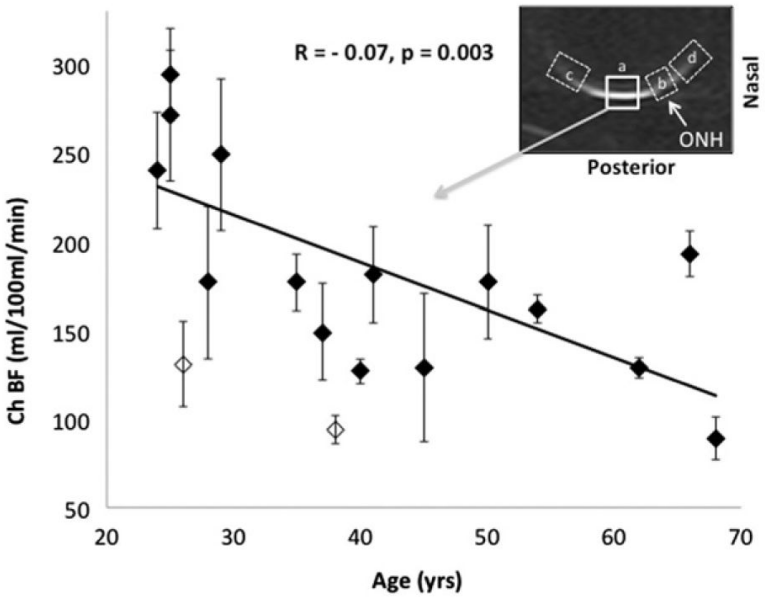

FIGURE 4.

Correlation plot of choroidal blood flow (ChBF) versus age for the ROI "a" shown. ChBF versus age was statistically significant ($R = -0.7$, $p = 0.003$, $N = 15$) without the two open symbols, which represented two subjects with severe myopia. The regression line was obtained without these two subjects. If they were included, then $R = -0.54$, $p = 0.03$, $N = 17$. There was also significant age-dependent effect for the optic nerve head ROI (labeled as b). There were no significant age-dependent effects for the periphery ROIs (labeled as c and d). Results from ROIs b, c and d are not shown.

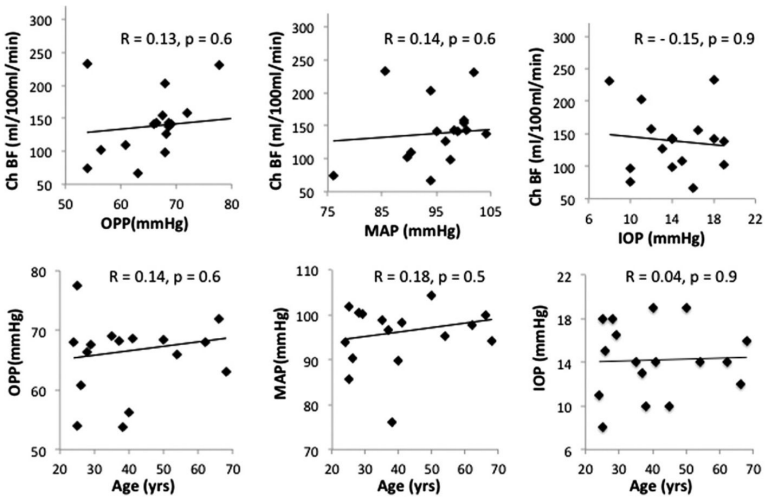

FIGURE 5.

Correlation plots of choroidal blood flow (ChBF) versus ocular perfusion pressure (OPP), mean arterial blood pressure (MAP), and intraocular pressure (IOP) for the ROI a (as shown in Figure 4). Correlation plots of OPP, MAP, and IOP versus age. Correlation plots show a trend but were not statistically significant ($p>0.05$).

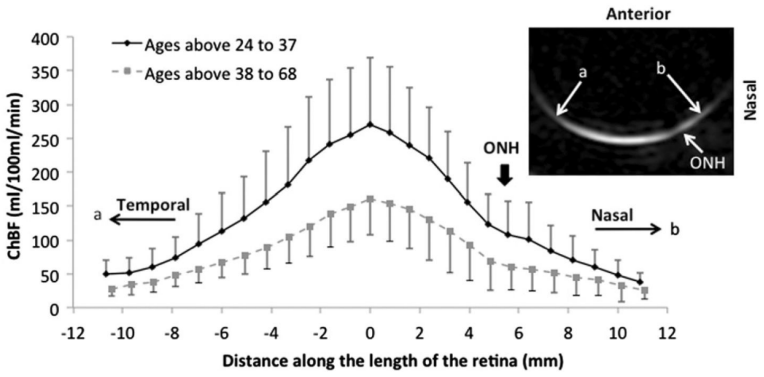

FIGURE 6.

BF profiles along the length of the retina from a to b. Subjects were divided into two groups (24–37-year-olds and 38–68-year-olds). Peak BF in the older group was lower than in the younger group (unpaired *t*-test $p<0.023$). Note that the slight shift on the x-axis between the two group is because different subjects had slightly different retinal curvatures while the MRI spatial resolution matrix is Cartesian. Thus, the distances from the fovea did not fall on the same Cartesian grids after linearization. Error bars are ±SD.